A Contactless Volumeter for Arm Volume and Circumference Measurement Using Depth Cameras for Early Detection of Lymphedema after Breast Cancer Surgery

Sopark Manasnayakorn
Department of Surgery
Faculty of Medicine
Chulalongkorn University
Bangkok, Thailand
sopark.m@chula.ac.th

Watchara Ruangsang
Department of Electrical Engineering
Faculty of Engineering
Chulalongkorn University
Bangkok, Thailand
watchara.knot@gmail.com

Panuwat Lertsithichai
Department of Surgery
Faculty of Medicine
Ramathibodi Hospital
Mahidol University
Bangkok, Thailand
panuwat.ler@mahidol.ac.th

Chatchai Sermpongpan
Department of Electrical and Computer Engineering
Faculty of Engineering
King Mongkut's University of Technology North Bangkok
Bangkok, Thailand
chatchai.s@eng.kmutnb.ac.th

Abstract— **Breast cancer is the most prevalent cancer among females, often leading to complications like lymphedema. Current detection methods for lymphedema following breast cancer surgery are imprecise and time-consuming. We present a cost-effective and user-friendly contactless arm volumeter for accurate lymphedema detection. Our volumeter utilizes six depth cameras to capture a 3D arm representation. By combining the recorded depth points from multiple angles, we measure arm circumference and volume accurately. In a study with 25 volunteers, we compared volumeter measurements with standard methods using a tape measure and water displacement. The intraclass correlation coefficient (ICC) assessed agreement and reliability. Results showed strong consistency agreement (ICC: 0.981 for volume, 0.868 for upper arm circumference, and 0.933 for lower arm circumference) and absolute agreement (ICC: 0.975 for volume, 0.866 for upper arm circumference, and 0.895 for lower arm circumference). Reliability was high (ICC: 0.993 for right arm volume, 0.975 for left arm volume, 0.988 for right arm circumference, 0.975 for left arm circumference (upper arm), and 0.948 for right arm circumference, 0.933 for left arm circumference (lower arm)). Our contactless arm volumeter is a reliable and cost-effective solution for detecting lymphedema after breast cancer surgery. Its ease of use and accuracy enable timely detection and treatment, potentially improving patient outcomes.**

Conflict of interest statement: Manasnayakorn S, Ruangsang W and Sermpongpan C are listed as inventors on the pending patent (2301000770) filed by CUIP for the volumeter described in this article.

Keywords—volumeter, lymphedema, depth camera, point cloud, breast cancer, breast cancer surgery, lymphatic obstruction

I. Introduction

Breast cancer is the most common cancer among women worldwide [1]. While surgical treatments have been de-escalated in recent decades, complications such as lymphedema still remain. Lymphedema is a medical condition characterized by the accumulation of lymph fluid, particularly in the arm, which can occur after breast cancer surgery. This condition arises due to fibrotic processeses obstructing the lymphatic vessels in the armpit following the surgery. Detecting and treating lymphedema early are of paramount importance to achieve successful outcomes [2].

In the field of lymphedema detection, current methods primarily rely on physical measurements of arm volume or circumference. However, these existing techniques, such as tape-based circumference measurement and water displacement for volume determination, suffer from significant drawbacks, including time-consuming procedures and the need for external assistance in the case of arm circumference measurement for breast cancer patients [3]. To address these limitations, various alternative techniques have been explored for arm volume measurement. For several decades, plethysmography has served as a valuable method for measuring changes in volume. Different types of plethysmography, such as fluid displacement, mercury strain gauge and capacitance plethysmography, have been described. Although this technique detects changes in volume rather than absolute volume, it provides a useful example for our volumeter [4]. Another method involves the use of Perometer®, an optoelectronic limb volumeter that employs infrared light emitting diodes (LED) integrated into a measuring frame [5]. Another approach utilizes a "structured-light" sensor to detect arm volume [6]. Both techniques have demonstrated satisfactory levels of accuracy in arm volume measurement. Furthermore, Ohberg introduced a volumeter that employs three 3D cameras for this purpose [7]. In a

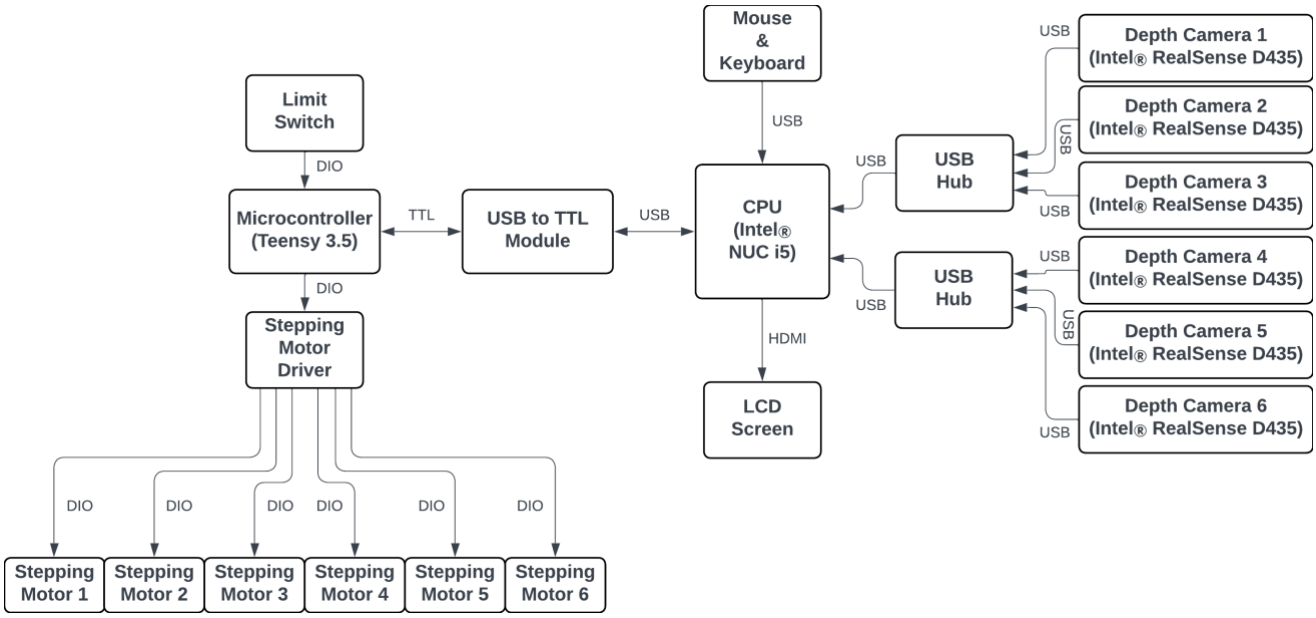

Fig. 1. A schematic diagram of the contactless volumeter measurement system (CPU: Central Processing Unit; LCD: Liquid Crystal Display; USB: Universal Serial Bus; TTL: Transistor-Transistor Logic; DIO: Digital Input/Output; HDMI: High-Definition Multimedia Interface)

similar way, Ono employed a 3D camera to accurately measure leg volume [8].

Bioimpedance spectroscopy (BIS) has emerged as a valuable technique in the measurement of arm edema, offering objective and non-invasive assessments in both clinical and research settings. By analyzing changes in tissue impedance across a range of frequencies, BIS provides a comprehensive evaluation of the affected limb. This multi-frequency approach allows for the characterization of various tissue compartments, such as extracellular fluid and cellular components, leading to a more comprehensive understanding of the edematous condition. BIS enables longitudinal monitoring of patients through periodic measurements. Early detection of lymphedema using BIS, coupled with timely treatment, has been shown to reduce the incidence of lymphedema compared to tape measurements [9]. However, it is crucial to ensure accurate and reproducible results by employing proper electrode placement and standardized measurement protocols.

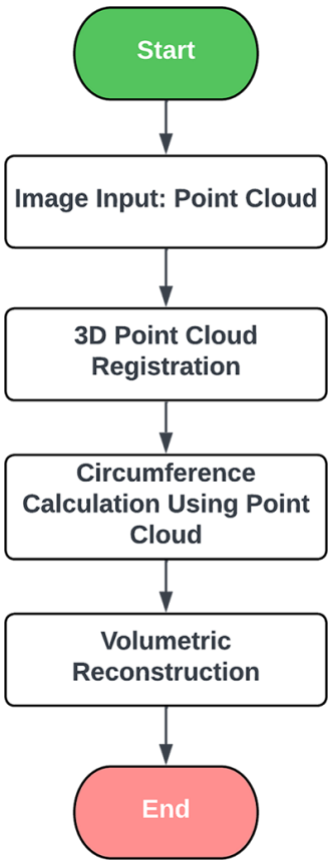

Fig. 2. A schematic diagram of 3D arm point cloud obtaining process

While Magnetic Resonance Imaging (MRI) provides detailed imaging of soft tissues, allowing accurate measurements of fluid accumulation and tissue changes in the affected limb, it is relatively costly and less accessible compared to other modalities [10]. As a result, there is a need for innovative solutions that address the practical challenges and limitations associated with current methods. A groundbreaking approach involves the development of a contactless volumeter that utilizes depth cameras. This novel volumeter aims to provide accurate measurements of arm circumference and volume, while mitigating the issues encountered with existing techniques. By leveraging the capabilities of 3D cameras, this invention has the potential to revolutionize lymphedema assessment by offering a contactless, efficient, and accurate solution.

Overall, the development of a volumeter utilizing 3D cameras holds significant promise in overcoming the challenges posed by current methods of arm volume measurement in lymphedema patients. Its potential to provide precise and accessible assessments highlights the importance of further exploring and advancing this innovative technology.

II. Methods

In order to account for the irregular contour of the hand, it was excluded from the measurements conducted using the contactless arm volumeter. The volumeter was designed with six depth cameras (Intel® RealSense™ D435, © Intel Corporation, CA, USA) arranged in a circular configuration,

Fig. 3. The final 3D image of arm, obtaining from 6 depth cameras

positioned vertically with each camera facing the center. These cameras were mounted on a motor-driven sliding rail for controlled movement. Each of the 6 cameras has the ability to slide and adjust its position independently. This movement is made possible through the use of timing belts, which are driven by stepper motors. By sending specific position values to each motor and referencing them from the home position, precise control over the camera's position can be achieved (Fig. 1).

The steps in 3D arm point cloud obtaining process are as follows: (Fig. 2)

A. Image Input

The measurement process involved capturing two sets of depth point recordings from different angles: the first set at the beginning of the scanning process and the second set at the midlength of the arm. These recordings produced point clouds representing the surface of the arm in (x,y,z) coordinates. To align these point clouds, the coordinates from each camera were converted to homogeneous coordinates (x,y,z,1) and represented as a 3D matrix.

B. 3D Point Cloud

The alignment of multiple sets of 3D point cloud data to form a coherent shape is referred to as 3D point cloud registration. This registration process aims to find the corresponding point cloud captured from each depth camera and transform each set of point cloud to achieve agreement between the corresponding point clouds. The registration process can be divided into two steps: coarse registration and fine registration.

1) Coarse Registration

The coarse registration step involves aligning the six sets of point clouds by applying translation and rotation transformations. The transformation equation used in this step is defined as:

$$P_i = RP_i + t \tag{1}$$

Here, P_i represents the point cloud coordinates (x,y,z), R is the camera rotation matrix and t is the camera translation vector

2) Fine Registration

The fine registration step is performed after the coarse registration, aiming to further refine the alignment of the point cloud sets. In this step, the Iterative Closest Point (ICP) algorithm is employed to find the translation vector and rotation matrix that minimize the distance between the corresponding points in the two point cloud sets. The fine registration process involves the following two steps:

- Finding the corresponding points between the reference point cloud and the target point cloud at the current transformation matrix. These corresponding points represent the closest matching points between the two sets of point clouds.

$$\kappa = \{(p, q)\} \tag{2}$$

- Once the corresponding points are identified, the transformation matrix (T) is determined to align (rotate) and move (translate) the target point cloud towards the reference point cloud. The transformation equations used in this step are:

$$T(p) = Rp + t \tag{3}$$

$$p = T(q) \tag{4}$$

Here, T represents the transformation matrix, R is the rotation matrix, t is the translation vector, p is the point cloud coordinates (x,y,z) and q represents the corresponding point cloud coordinates.

The fine registration process is iteratively repeated until the error between the point cloud sets falls below a threshold or reaches the maximum number of iterations. The error between the point cloud sets is calculated using the following formula:

$$E(T) = \sum_{(p,q)\in\kappa} \|p - Tq\|^2 \tag{5}$$

Overall, the contactless arm volumeter utilizes depth cameras and employs a registration process to align multiple sets of point clouds, allowing for accurate measurements of arm volume and circumference. The combination of coarse and fine registration steps ensures the precise alignment of point cloud data (Fig. 3).

C. Circumference Calculation Using Point Cloud:

In order to analyze the arm's irregular circular shape, a best-fit circle was determined from the cross-sectional view of the 3D point cloud. This circle served as a representation of the arm's contour and allowed for the calculation of circumference and cut surface area. The best-fitting circle (Fig. 4) was obtained by solving the equation:

$$(x_i - x_c)^2 + \left(y_i - y_c\right)^2 = r^2 \tag{6}$$

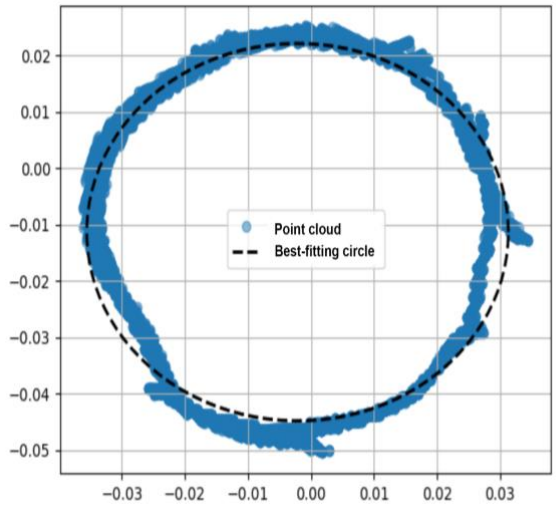

Fig. 4. The best-fit circle was determined from the cross-sectional view of the 3D point cloud as a representation

Fig. 5. Measuring arm in a volunteer

where x_i and y_i are the positions on the X and Y axes, respectively, of a point of interest in the point cloud, x_c and y_c represent the position on the X and Y axes, respectively, of the center point of the circle and r represents the radius of the circle.

D. Volumetric Reconstruction from Surface Data

Considering the cylindrical shape of the arm, the volume of the object can be calculated using the formula

$$V = Ah \tag{7}$$

where V is the volume, A is the cross-sectional area and h is the height of the object. However, the arm's shape may have varying cross-sectional areas along its length. In such cases, an approximate volume can be estimated by dividing the arm into smaller subregions with equal heights. The volume can then be calculated using the formula:

$$V = A_1 h_s + A_2 h_s + A_3 h_s + \cdots + A_n h_s \tag{8}$$

or

$$V = \sum_{i=1}^{n} A_i h_s \tag{9}$$

where V is the volume of the object, A_i is the cross-sectional area or the area of the sliced image for each subregion, h is the total height of the object, n is the number of subdivided sections and h_s is the height of each section, which is equal to $\frac{h}{n}$.

In summary, the volumetric reconstruction of the arm involves determining the best-fit circle from the point cloud to calculate the circumference, and dividing the arm into smaller sections to estimate the volume by summing the cross-sectional areas of each section multiplied by their respective heights.

The project received approval from the institutional review board (IRB), and all volunteers provided informed consent.

Arm measurements were taken starting 5 cm above the elbow and extending to the farthest measurable part of the forearm, typically just above the wrist (excluding the hand). To capture arm volume, the volumeter was used, taking four measurements. For each measurement, we calculated the circumferences at both ends of the specified sections, resulting in four measurements each. Additionally, we performed standard measurements using tape and water displacement twice, resulting in two measurements each. We model the measurement of arm size using 3 linear mixed models, one for each arm size measure: arm volume, upper and lower arm circumference. The linear mixed model is of the form

$$V_{ijhk} = v + \beta_k + u_i + w_{ij} + e_{ijhk};$$
$$u_i \sim N(0, \sigma_u^2) \perp W_{ij} \sim N(0, \sigma_w^2) \perp e_{ijhk} \sim N(0, \sigma_e^2) \tag{10}$$

Here, V_{ijhk} is the arm size measurement for arm j (Right or Left) of subject i (25 subjects) measured using the method k (2 methods) for the occasion h (2 repeated measurements). u_i, w_{ij}, e_{ijhk} are the random subject effect, random arm effect and residual error, respectively, with the corresponding variance components $\sigma_u^2, \sigma_w^2, \sigma_e^2$. All the random components are independent of one another and we assume no interaction effects between subject and method. v is the average arm size for the standard measurement method and β_k are the fixed measurement method effects: β_1 is the average size difference between volumeter and standard methods, and $\beta_0 = 0$ by definition.

If the estimated variance components of the above mixed model are $\hat{\sigma}_u^2$, $\hat{\sigma}_w^2$, $\hat{\sigma}_e^2$ and the variation in the values of the estimated fixed effects $\hat{\beta}_k$ is written as $var(\hat{\beta})$ where

$$var(\hat{\beta}) = \frac{\sum_k (\hat{\beta}_k - \hat{\beta}_\cdot)^2}{K-1}; \ \hat{\beta}_\cdot = \frac{\sum_k \hat{\beta}_k}{K} \tag{11}$$

and K is the number of measurement methods, here $K = 2$, then the estimated consistency agreement, a form of intraclass correlation coefficient (ICC), is

$$consistency\ agreement = \frac{\hat{\sigma}_u^2 + \hat{\sigma}_w^2}{\hat{\sigma}_u^2 + \hat{\sigma}_w^2 + \hat{\sigma}_e^2} \tag{12}$$

and the estimated absolute agreement is

$$absolute\ agreement = \frac{\hat{\sigma}_u^2 + \hat{\sigma}_w^2}{\hat{\sigma}_u^2 + \hat{\sigma}_w^2 + var(\hat{\beta}) + \hat{\sigma}_e^2} \tag{13}$$

The consistency agreement ignores variability due to measurement method, $var(\hat{\beta})$, and is a useful indicator of the consistency of ranking of arm size, while absolute agreement indicates agreement of actual arm size values, not just the ranks, and hence is absolute. Absolute agreement can be interpreted in the present study as the accuracy of the volumeter against the standard measurement. We report both consistency and absolute agreements when the 2 measurement methods are compared. For the reliability, or precision, of any given method to consistently reproduce the same or similar measurement values every time, only consistency-type agreement was obtained. Stata statistical software version 14.2 (Stata Corp, College Station, TX, USA) was used for all statistical analyses. In the present report, 95% Confidence Intervals (95% CI) are available only for the consistency agreement.

III. Results and Discussion

Twenty-five volunteers, including 15 females and 10 males, participated in the study, with ages ranging from 21 to 61 years. Among them, 23 were right-handed, while one male and one female were left-handed.

For the right arm, the fourth measurement data from the volumeter were missing for five volunteers, and for the left arm, three measurement data from the volumeter were missing for one volunteer. As a result, we had 292 measurements available for analysis.

Results of the analysis are provided in the tables below. We have three separate analyses for the 3 arm size measurements: arm volume, upper arm circumference, and lower arm circumference. In Table 1, we present estimates of

parameters in the linear mixed model for the arm volume measurements only. This is to show how these estimates correspond to the statistical model presented earlier, and to show the components used for the agreement estimates. For other arm size measurements, these parameters estimates are not shown. Table 2 shows the agreement between the volumeter and standard methods for the 3 arm size measurements separately, and Table 3 shows the reliability of both the volumeter and the standard methods for the 3 arm size measurements.

TABLE I. ESTIMATES OF PARAMETER VALUES IN THE LINEAR MIXED MODEL FOR ARM VOLUME MEASUREMENT ONLY (N = 292)

Parameter	Estimate	95% CI*
Average arm volume, by standard method, $\hat{v}$ (mL)	935.6	844.6 to 1026.6
Average difference between volumeter & standard method, $\hat{\beta}_1$ (mL)	26.4	18.5 to 34.4
Subject variance, $\hat{\sigma}_u^2$	52,212.9	29,501.7 to 92,408.0
Side of arm (i.e., right or left side) variance, $\hat{\sigma}_w^2$	2,879.9	1,593.9 to 5,203.3
Residual error variance, $\hat{\sigma}_e^2$	1,069.3	894.8 to 1,227.9
Fixed effect (measurement method) variance, $var(\hat{\beta})$	349.1	-

*95% CI: 95% Confidence Interval

TABLE II. ESTIMATES OF AGREEMENT BETWEEN VOLUMETER AND STANDARD ARM SIZE MEASUREMENTS (N = 292)

Arm size measurements	Agreement estimate	95% CI*
Arm volume		
Consistency agreement	0.981	0.967 to 0.989
Absolut agreement	0.975	-
Upper arm circumference		
Consistency agreement	0.868	0.786 to 0.922
Absolut agreement	0.866	-
Upper arm circumference		
Consistency agreement	0.933	0.891 to 0.960
Absolut agreement	0.895	-

*95% CI: 95% Confidence Interval

TABLE III. ESTIMATES OF RELIABILITY (AMONG REPEATED MEASUREMENTS) OF THE 2 MEASUREMENT METHODS FOR THE 3 ARM SIZE MEASUREMENTS

Arm size measurements	Reliability estimate	95% CI*
Arm volume		
Standard method: right arm (n = 50)	0.975	0.946 to 0.989
Standard method: left arm (n = 50)	0.994	0.987 to 0.997
Volumeter: right arm (n = 50)	0.993	0.984 to 0.997
Volumeter: left arm (n = 49)**	0.975	0.945 to 0.989
Upper arm circumference		
Standard method: right arm (n = 50)	0.998	0.997 to 0.999
Standard method: left arm (n = 50)	0.996	0.992 to 0.998
Volumeter: right arm (n = 50)	0.988	0.974 to 0.994
Volumeter: left arm (n = 49)**	0.975	0.945 to 0.988
Upper arm circumference		
Standard method: right arm (n = 50)	0.997	0.993 to 0.999
Standard method: left arm (n = 50)	0.998	0.995 to 0.999
Volumeter: right arm (n = 50)	0.948	0.890 to 0.976
Volumeter: left arm (n = 49)**	0.933	0.860 to 0.969

*95% CI: 95% Confidence Interval; **There was 1 missing observation per measure for one left arm in one subject

The comparison between the volumeter measurements and standard measurements revealed a high level of agreement and reliability (Table 2). The agreement between the volumeter and standard measurements indicated a high accuracy of the volumeter against the standard measurements, with consistency and absolute agreement values of 0.981 and 0.975, respectively, for the arm volume, which are considered acceptable for clinical applications [11]. The consistency and absolute agreements were 0.868 and 0.866, respectively, for the upper arm circumference, and 0.933 and 0.895 for the lower arm circumference, demonstrating good accuracy for both these measurements as well. The corresponding 95% Confidence Intervals (95% CI) were all sufficiently narrow, indicating rather precise estimation. The reliability or precision of the measurement methods was also very high, as shown in Table 3. For example, the volumeter itself was highly reliable, with a reliability of well over 0.9 for all arm size measurements, regardless of the side of the arm. Their 95% CI's were very narrow as well. In other words, the measurements made by the volumeter should be highly reproducible. Despite these promising results, it remains to be seen how reliable the volumeter will be within the context of upper limb lymphedema, and a validation study on actual patients will be necessary.

The accuracy of the volumeter for volume measurement can be determined using the following equation:

$$\%\ accuracy = 100 - \%\ error \tag{14}$$

where

$$\%\ error = relative\ error \times 100 \tag{15}$$

and

$$relative\ error = \left|\frac{x_{mea} - x_t}{x_t}\right| \tag{16}$$

when x_{mea} is measured value, and x_t is true value. By applying these equations, the accuracy of the volumeter for volume measurement is found to be 96.25%. This is again considered acceptable for clinical applications [11].

Comparing the performance of our method with existing similar techniques is somewhat challenging due to differences in study designs. Nonetheless, we did find a similar product reported by Ohberg et al [7]. In their study, the researchers observed a tendency towards overestimating arm volume by 45.25 mL. However, this difference was not statistically significant when compared to standard measurements. Similarly, our study also identified a comparable trend, with an overestimation of 26.4 mL. Regrettably, the authors did not provide the measured arm volume, preventing us from calculating their overestimation percentage. Additionally, the report did not mention the accuracy of their method. Nevertheless, we found that the agreement between each volumeter and the standard methods for arm volume measurement is comparable.

The volumeter efficiently obtained arm circumferences on both ends and arm volume simultaneously, with each measurement completed in less than 10 seconds. In contrast, the corresponding measurements using standard methods typically required at least 10 minutes. Although we did not include the measurement time as an outcome, this substantial time-saving advantage could proved highly advantageous in outpatient clinics, allowing for early detection of lymphedema. Moreover, the contactless nature of the measurement method aligns perfectly with the current pandemic era, minimizing physical contact and mitigating potential infection risks.

In terms of cost-effectiveness, the arm volumeter proves to be an economical alternative compared to optoelectronic volumeters or magnetic resonance imaging (MRI) measurements. The total budget for developing the arm volumeter was less than ฿500,000 (approximately $14,000), making it more accessible and feasible for widespread use in

clinical settings. This affordability opens up possibilities for utilizing the volumeter in postoperative breast cancer surgery to aid in the early detection of lymphedema.

IV. Conclusion

The volumeter utilizing depth cameras provides highly accurate measurements of arm circumference and volume, with intraclass correlation coefficients as high as 0.981. Moreover, it is cost-effective, convenient, and user-friendly, making it readily acceptable for daily use. This contactless volumeter serves as a valuable tool for detecting lymphedema after breast cancer surgery, resulting in better outcomes through prompt treatment. The future development of the next-generation volumeter will address the hand-measuring limitation and further enhance its capabilities.

Acknowledgment

The authors would like to express our heartfelt gratitude to the following organizations and individuals, without whom this project would not have been possible:

1. This research is funded by Chulalongkorn University under grant number CU_GI_62_01_30_01. The authors would like to express their gratitude for this financial support, which played a vital role in the successful completion of the project.
2. iRAP (Invigorating Robot Activity Project, Faculty of Engineering, King Mongkut's University of Technology North Bangkok): The authors extend our sincere appreciation to iRAP for generously providing the necessary equipment and workshop space. This invaluable support played a crucial role in the successful execution of this project.
3. Mr. Tanawit Sinsukudomchai, Mr. Theerawath Phetpoon, Mr. Chareef Jeaputea, Mr. Tula Chewachatreekasem, and Mr. Sippakorn Chatjariyawet: The authors wish to extend our warmest thanks to these individuals for their kind and indispensable assistance during the building phase of the volumeter. Their expertise and dedication greatly contributed to the project's progress and outcomes.
4. Ms. Pitima Kurimoto: The authors are deeply appreciative of Ms. Pitima Kurimoto for her exceptional administrative support and dedication to data collection. Her efforts were instrumental in ensuring the smooth coordination and organization of the project.

References

[1] H. Sung, J. Ferlay, R. L. Siegel, M. Laversanne, I. Soerjomataram, A. Jemal, and F. Bray, "Global Cancer Statistics 2020: GLOBOCAN Estimates of Incidence and Mortality Worldwide for 36 Cancers in 185 Countries," *CA Cancer J Clin,* vol. 71, no. 3, pp. 209-249, May, 2021.

[2] A. Soran, T. Ozmen, K. P. McGuire, E. J. Diego, P. F. McAuliffe, M. Bonaventura, G. M. Ahrendt, L. DeGore, and R. Johnson, "The importance of detection of subclinical lymphedema for the prevention of breast cancer-related clinical lymphedema after axillary lymph node dissection; a prospective observational study," *Lymphat Res Biol,* vol. 12, no. 4, pp. 289-94, Dec, 2014.

[3] J. Lette, "A simple and innovative device to measure arm volume at home for patients with lymphedema after breast cancer," *J Clin Oncol,* vol. 24, no. 34, pp. 5434-40, Dec 1, 2006.

[4] T. Tamura, "5.05 - Blood Flow Measurement," *Comprehensive Biomedical Physics*, A. Brahme, ed., pp. 91-105, Oxford: Elsevier, 2014.

[5] A. W. Stanton, J. W. Northfield, B. Holroyd, P. S. Mortimer, and J. R. Levick, "Validation of an optoelectronic limb volumeter (Perometer)," *Lymphology,* vol. 30, no. 2, pp. 77-97, Jun, 1997.

[6] R. Buffa, E. Mereu, P. Lussu, V. Succa, T. Pisanu, F. Buffa, and E. Marini, "A new, effective and low-cost three-dimensional approach for the estimation of upper-limb volume," *Sensors (Basel),* vol. 15, no. 6, pp. 12342-57, May 26, 2015.

[7] F. Ohberg, A. Zachrisson, and A. Holmner-Rocklov, "Three-dimensional camera system for measuring arm volume in women with lymphedema following breast cancer treatment," *Lymphat Res Biol,* vol. 12, no. 4, pp. 267-74, Dec, 2014.

[8] K. Ono, R. Koike, Y. Miyazaki, M. Masujima, K. Ogawa-Ochiai, and N. Tsumura, "A Circumference-Measurement Method Using a Model of a Leg and a 3D Camera," *Annu Int Conf IEEE Eng Med Biol Soc,* vol. 2021, pp. 1376-1379, Nov, 2021.

[9] S. H. Ridner, M. S. Dietrich, J. Boyages, L. Koelmeyer, E. Elder, T. M. Hughes, J. French, N. Ngui, J. Hsu, V. G. Abramson, A. Moore, and C. Shah, "A Comparison of Bioimpedance Spectroscopy or Tape Measure Triggered Compression Intervention in Chronic Breast Cancer Lymphedema Prevention," *Lymphat Res Biol,* vol. 20, no. 6, pp. 618-628, Dec, 2022.

[10] T. C. Case, C. L. Witte, M. H. Witte, E. C. Unger, and W. H. Williams, "Magnetic resonance imaging in human lymphedema: comparison with lymphangioscintigraphy," *Magn Reson Imaging,* vol. 10, no. 4, pp. 549-58, 1992.

[11] L. G. Portney, Foundations of clinical research: applications to evidence-based practice, 4th ed., Philadelphia: F. A. Davis Company, 2020